Chapter 1

Introduction

"*Great is the Earth, and the way it became what it is. Do you imagine it is stopped at this?*"

by Walt Whitman

This chapter presents a general overview and motivation of the thesis work. The chapter discusses the evolution and tectonic setting of the Himalaya along with its major fractures (thrusts), subsequent seismicity, and seismic gaps. It also includes the objectives and the scope of the present work.

Contents

1.1 Overview and motivation

The plate tectonics theory suggests that the Earth's upper crust is broken into several plates, namely oceanic and continental plates. These plate boundaries either converge or diverge or transform to each other. The convergent boundaries create either a mountain belt, subduction zone, or a trench; the divergent boundaries form either mid-ocean ridges, rift valleys, or volcanoes; and the transform boundaries create fissure volcanoes or earthquakes. The long-term convergence of the India-Eurasia plate collision forms the Himalayan mountain belt, resulting into enormous strain accumulation along the north-dipping detachment zone of the Himalayan orogen [87, 259, 291]. This detachment zone consists of three megathrusts and a décollement [289, 321]. The fault system has produced many devastating earthquakes in the past and has the potential to generate large events in the future [93, 276].

Crustal shortening imposed by the plate collision on the interseismically locked and seismically active faults ultimately leads to strain accumulation, which is subsequently released in terms of earthquakes [253]. The quiescence of significant earthquakes along the Himalayan arc for the past hundred years may induce major to great earthquakes in the future. The April 25, 2015 Gorkha earthquake (M_w=7.8) was a dramatic reminder of such future incidence [62]. The Himalayan arc has also experienced some destructive earthquakes in the past, namely the April 04, 1905 Kangra earthquake (M_w=7.8), January 15, 1934 Bihar-Nepal earthquake (M_w=8.4), August 15, 1950 Assam earthquake (M_w=8.6), and the October 08, 2005 Kashmir earthquake (M_w=7.6) [8, 17, 128]. Apart from these earthquakes, there have been evidences of at least hundreds of large to moderate events in the Himalayan orogen in the past century [30, 268, 321]. In addition, the population density along the Himalaya and its adjacent regions has increased since these earthquakes strike, increasing potential for catastrophic damage and loss in upcoming earthquakes. Therefore, it is of great importance to understand the distribution of large historical earthquakes and consequent seismic budget along the Himalayan arc [34].

Bilham et al. (2001) [34] (Fig. 1.1) divided the Himalayan arc into 10 seismogenic regions to estimate potential magnitude and slip of future earthquakes based on Global Positioning System (GPS) studies, geological investigations, and historical seismicity. However, due to the occurrence of two recent large earthquakes in 2005 (Kashmir earthquake) and in 2015 (Gorkha earthquake), Bilham (2019) [30] (Fig. 1.1) re-estimated the magnitude and slip potential of the Himalayan arc along 15 seismogenic segments.

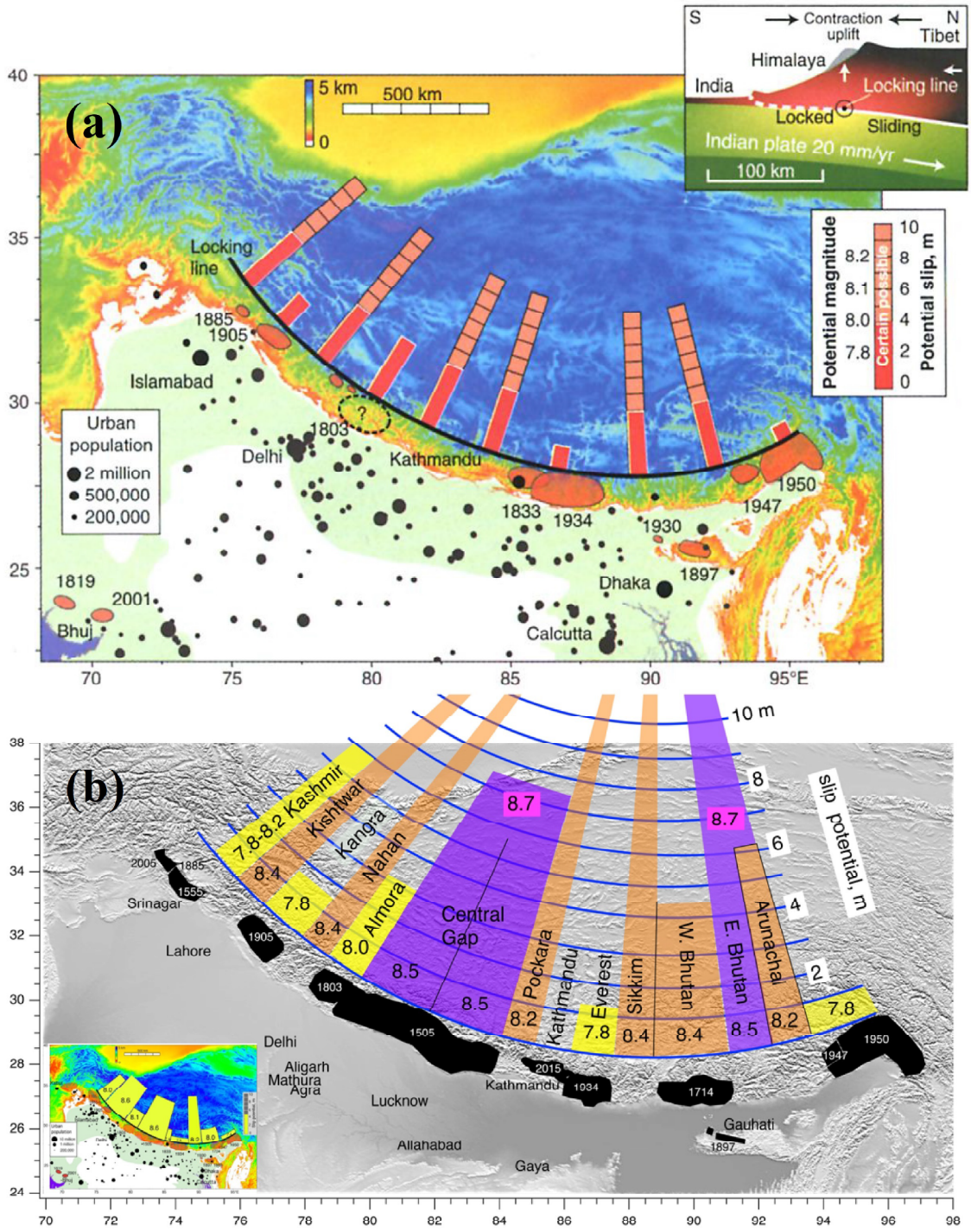

Fig. 1.1: (a) Potential magnitude and slip potential along the Himalayan arc (Bilham et al., 2001 [34]); (b) re-estimated potential slip along the Himalayan arc (Bilham, 2019 [30]).

Continuous measurements of crustal deformation and plate motion along the Himalayan arc can help us to understand the kinematics of the megathrust system and identification of the relatively high seismic potential zones. Several methods, such as the geodetic investigation of crustal deformation, geological and paleoseismological findings of mapped faults, seismological observations, and geophysical techniques have been proposed to analyze the dynamic behavior of crustal deformation and associated earthquake potential along the Himalayan arc [20, 35, 161, 310]. Among these different techniques, geodetic observations can provide precise estimate of horizontal signals up to mm level accuracy, allowing us to derive the spatial distribution of strain rates and fault kinematics along plate boundaries [253].

In light of the above, the present thesis has focused on measuring and modeling of the ongoing crustal deformation along the Himalayan arc based on a dense GPS network comprising regional and published horizontal velocities. The surface velocities are used to derive interseismic strain accumulation rate and fault slip rate along the megathrust system. The strain accumulation rate provides moment build-up rate and if compared with the moment release rate, it can provide current earthquake potential for an area [55]. On the other hand, the slip rate and the fault geometry estimates enable us to determine whether the fault is presently locked or it is interseismically active. This information is indispensable to re-construct the regional-scale crustal deformation and its implication on future seismic hazard [20, 154, 277, 316]. In addition to the geodetic analysis, a statistical investigation based on the concept of natural times is also carried out to determine the current state of seismic hazard in a dozen populous cities along the Himalayan subcontinent. Both geodetic and statistical methods of seismic hazard assessment are related to the concept of elastic rebound.

1.2 Evolution of the Himalaya

Geography and tectonics of the mighty Himalaya and its adjacent regions are mainly the results of persistent collision of Indian and Eurasian plates since ∼50 Ma. The Eurasian plate is a ‘composite continent’in which several landmasses have collided and joined over the past ∼800 Ma (Fig. 1.2) [217]. Most of these landmasses are older than ∼200 Ma [100]. The Indian plate is the most recent addition of the Eurasian plate, joining the continent along the front of around ∼2400 km [1, 217].

Separated from the supercontinent Gondwana around ∼120 Ma, the Indian plate moved about ∼5000 km towards the Eurasian plate around 71 Ma at a rate of 15−20 cm/yr (Fig. 1.2) [175, 217, 257]. However, since ∼ 40 Ma, the India-Eurasia collision has slowed down, but not stopped, and the Indian plate is continuously marching northward (Fig. 1.2) [57, 58, 174]. Several hypotheses have been proposed to understand what has happened to the deformed crust after the two plates collided [28, 51, 293]. One mechanism suggests that the Indian plate is subducting underneath the Tibetan Plateau [28]; the second indicates that the Indian plate acts as a 'wedge', splitting the Eurasian plate and pushing Indochina out to the west; the third is orogeny – the thrusting and layering of the continental crust that move upward to create mountains [28, 51, 293]. All three hypotheses have been considered critical for the India-Eurasia collision, though the last one is widely accepted because it introduces the concept of spectacular mountain belt generation [28, 100, 222, 239, 258].

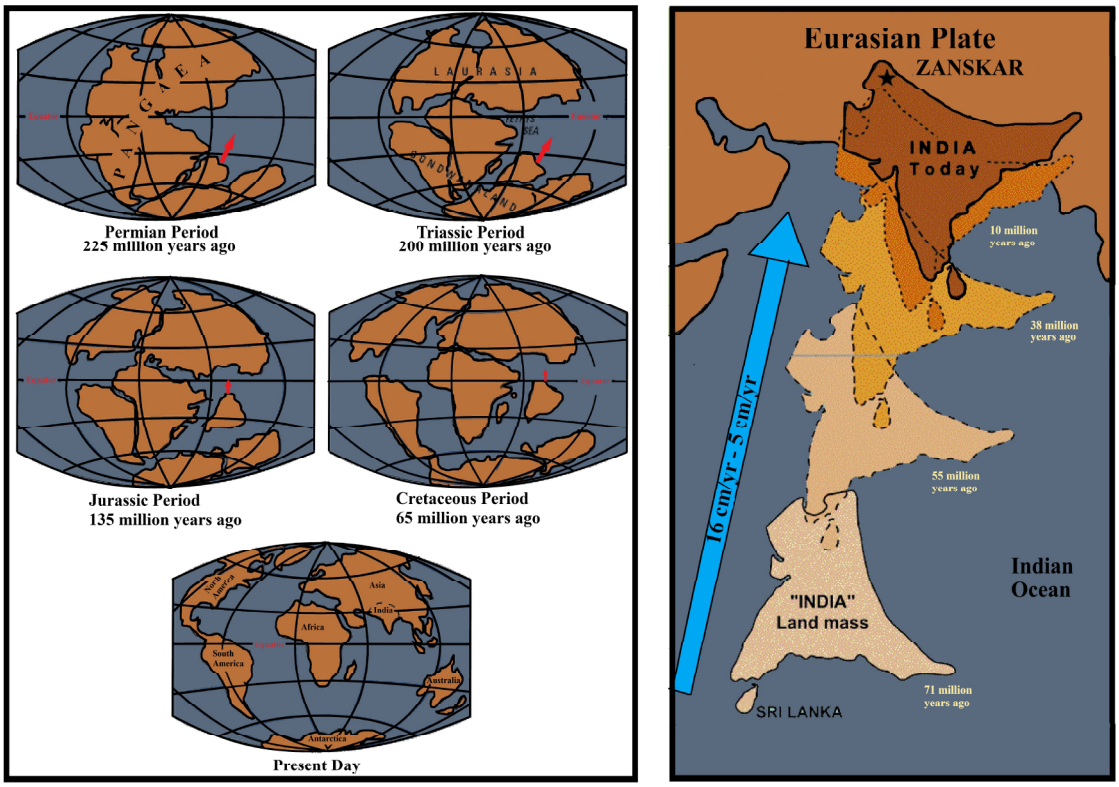

Fig. 1.2: Evolution of the Himalaya: the left panel shows how Pangaea broke into various pieces of continents, whereas the right panel presents the persistent motion of the Indian plate towards the Eurasian plate (source: www.usgs.gov).

The Himalayan mountain belt, formed due to the continuous convergence between

Indian and Eurasian plates, exhibits long-term evidence of thrusting and layering [100, 222, 239]. Previous studies suggest that the Tibetan Plateau and other adjacent regions of compression absorb half of the India-Eurasia plate convergence [20, 173, 321]. The remaining shortening has been accommodated by shoving Mongolia and China in the eastward direction, away from the path of the Indian plate, such as toothpaste squeezed from a tube [60, 100, 166, 196, 222, 239, 258]. As a consequence, mountains, plateaus, faults, landforms, and seismicity in the Himalaya and its adjacent regions, up to about thousands of kilometers away from the India-Eurasia suture zone, get affected by the Himalayan orogeny as India plows into Asia at a rate of ∼4−5 cm/yr [60, 196, 258, 321].

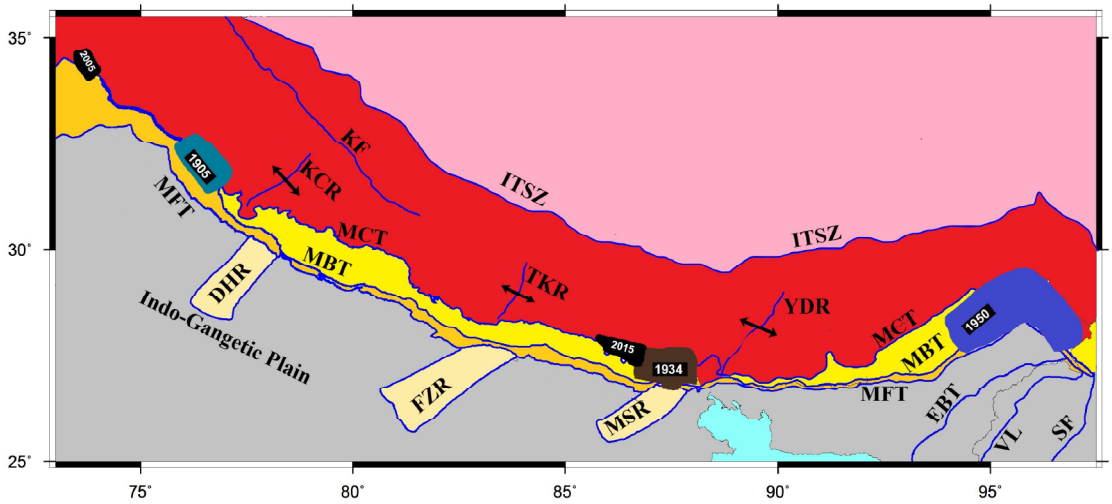

Fig. 1.3: Geological map of the Himalayan arc. Abbreviations are as follows: DHR, Delhi-Haridwar Ridge; EBT, Eastern Boundary Thrust; FZR, Faizabad Ridge; ITSZ, Indus-Tsangpo Suture Zone; KCR, Kaurik Chango Rift; KF, Karakorum Fault; MBT, Main Boundary Thrust; MCT, Main Central Thrust; MFT, Main Frontal Thrust; MSR, Munger-Saharsa Ridge; SF, Sagaing Fault; TKR, Thakola Rift; VL, Volcanic Line; YDR, Yodang Rift.

1.3 Tectonic or longitudinal classification

The ∼2400 km long Himalayan range along the northern tip of the Indo-Australian plate is bounded by the Namche Barwa range in the northeast direction and the Nanga-Parbat range in the northwest direction (Fig. 1.3) [271, 321]. The Himalayan arc and its surrounding areas are characterized by complex tectonics, showcasing various stages of geological and seismic activities. One of the significant aspects of the Himalayan arc is the

lateral continuity of its major tectonic events.

The Himalayan belt is divided into three parallel mountain ranges: the Siwalik or Outer Himalaya, Lesser Himalaya, and the Higher or Greater Himalaya, home to the mighty Everest (Fig. 1.4). From north to south, the width of these three ranges varies from ∼240 km to ∼320 km, whereas from west to east, they curve gently southeast in a sort of lopsided smile (Fig. 1.3) [87, 321]. Each of these geographical units of Himalaya is characterized by distinct stratigraphy and metamorphic rocks, and is separated from each other by large geological faults.

From the north, the Higher Himalaya is detached from the Tibetan sedimentary by the South Tibetan Detachment (STD); the Lesser Himalaya is separated from the Higher Himalaya by the Main Central Thrust (MCT); the Siwalik Himalaya is separated from the Lesser Himalaya by the Main Boundary Thrust (MBT); and the Indo-Gangetic Plain (IGP) is disconnected from the Siwalik Himalaya by the southernmost thrust, the Main Frontal Thrust (MFT) (Fig. 1.4) [259, 291].

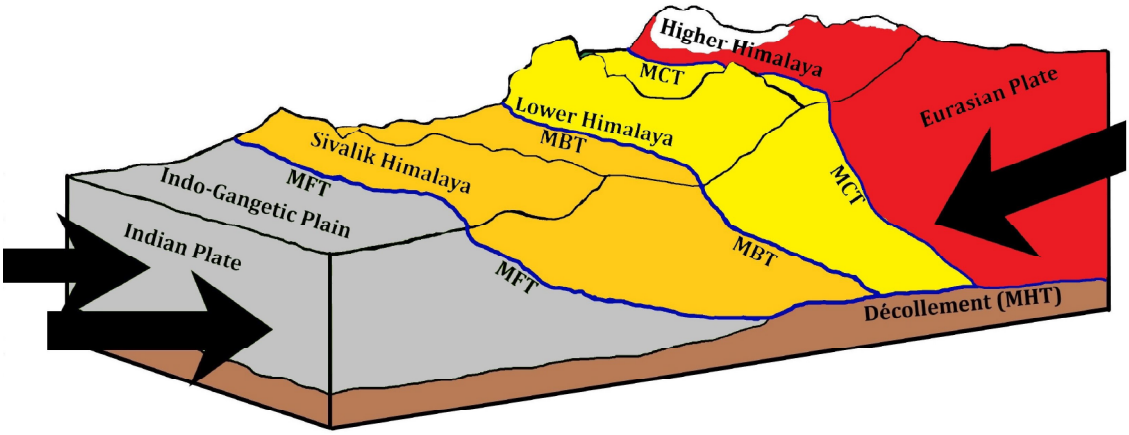

Fig. 1.4: Cross section of the Himalayan arc. Abbreviations are as follows: MBT, Main Boundary Thrust; MCT, Main Central Thrust; MFT, Main Frontal Thrust; MHT, Main Himalayan Thrust.

1.3.1 Higher Himalaya

The Higher Himalaya has evolved due to the ductile extrusion through earlier Miocene since 23 Ma. It is mostly composed of the colossal mass of strongly metamorphosed rocks (Fig. 1.4). The Higher Himalaya is also known as the 'Central Crystalline Axis' of the Himalayan province and it marks the orogenic uplift axis [321]. The Higher Himalaya

comprises high perennially snow-capped mountain ranges with an elevation of ∼3,000 m to ∼8,000 m. Some of the famous mountain peaks are the Mount Everest (8,849 m), K2 (8,611 m), Kanchenjunga (8,586 m), Lhotse (8,516 m), Nanga Parbat (8,126 m), Annapurna-I (8,100 m), Nanda Devi (7,925 m), Namcha Barwa (7,833 m), Kedarnath (6,940 m), Badarinath (6,798 m), Gangotri (6,400 m), and the Yamunotri (6,381 m) [321]. Further, the Higher Himalayan sedimentary rocks represent multiphase deformations corresponding to MCT [271]. Three north-south trending rifts have been identified along the Higher Himalaya. These are the Kaurik Chango Rift (KCR), Thakola Rift (TKR), and the Yadong Rift (YDR) (Fig. 1.3) [12]. Although the south extension of these rifts is not straightforward due to insufficiency of surface exposure, the segmentation of top sheeted Himalayan wedge from these rifts may play an important role in controlling the rupture extent of large Himalayan earthquakes [84].

1.3.2 Lesser Himalaya

The Lesser Himalayan belt is situated in the south of the Higher Himalaya bounded by the MBT and the MCT (Fig. 1.4) [321]. Older and geologically more complex, the Lesser Himalayan range has a width of 60−90 km. Although the Lesser Himalaya is not as highly elevated as the Higher Himalaya, it has elevations ranging from 3,700 m to 4,500 m [321]. Many peaks of the Lesser Himalaya are covered by thick layers of snow throughout the entire year. The rocks in this range comprise unmetamorphosed to low-grade metasediments primarily of Proterozoic age and categorized by some nappes of metamorphic rocks carried southwards over a long distance imbricate thrusting [149, 290]. Due to the increasing compression near the MCT, the metasedimentary rocks were squeezed and as a result, tightened folds appear, overturning and toppling the fold-thrust belt. This process gives rise to a duplex region composed of imbricated lithotectonic stacks [249, 289, 290]. More upward rooting of the folded sedimentary rocks opened in the south in the form of thrust sheets, klippe or nappe, e.g., the Almora Klippe, Shimla Klippe, Krol-Berinag Nappe, Kathmandu Nappe, and the Dadeldhura Nappe [64, 121, 288, 290]. These overthrust sheets mainly comprise metamorphic and granitic rock concordant with the underlying Precambrian sedimentary succession [290]. The rock units display a series of anticlines and synclines that are often clipped [3].

1.3.3 Siwalik Himalaya

The Siwalik Himalaya, also called the Churia Hills, is the youngest and the lowest southernmost mountain range along the Himalaya. It is bounded by the MBT in the north and the MFT in the south (Fig. 1.3) [290, 321]. The MFT also separates the Siwalik hills from the foreland of the IGP (Fig. 1.4). Parallel to the Lesser and the Higher Himalaya, this mountain range has an average elevation of 600−1,220 m and an average width of 10 to 48 km. The Siwalik mountain areas consist of sedimentary rocks deposited by the ancient Himalayan river in their channels and flood plains in the last 16 Ma to 1.5 Ma [291]. Lesser Himalayan terrains move further in the south along the boundary thrust (MBT), and fracture the Himalayan provinces into several tear faults and out of sequence faults [183]. Due to the long-term deformation along the Siwalik range, some pop-up structures (e.g., Shillong Plateau), fault scraps, piggyback basins (e.g., Deukhuri Dun, Chitwan Dun, Hetauda Dun, Pinjor Dun, Dehra Dun, Rapti-Dang Dun, and Kota-Pawalgarh Dun) have developed in these areas [15, 183].

1.3.4 Indo-Gangetic Plains

The region of modern alluvial sedimentary rocks of the Indo-Gangetic Plains (IGP) along the Himalayan front has evolved due to the flexure of the Indian plate by the heavy load of the Himalayan belt (Fig. 1.4) [321]. The basin comprises Indian foreland basement and Paleozoic platform sediments superimposed by Tertiary to Holocene sediments, mainly covered by alluvium. Sedimentary rocks of the basin are carried through the Himalayan rivers such as the Brahmaputra and the Ganges along with their subsidiaries. The fluvial deposits along the Himalayan front have $\sim$6 km thickness which decreases further in the south [320, 321]. The IGP is also the place of three large ridges, namely the Delhi-Haridwar Ridge (DHR), Faizabad Ridge (FZR), and the Munger-Saharsa Ridge (MSR) (Fig. 1.3) [87, 289]. The foreland basin provides a home for more than 200 million people and vast wildlife along with green forests (Fig. 1.1). The IGP fore-deep is not as seismically active as the Himalayan arc [225].

1.4 Latitudinal divisions

Along the strike of the Himalayan arc, it may also be divided into three broader segments: Northwest Himalaya ($\sim$71°– 80° E; Kashmir Sector, Himachal region, and Garhwal-Kumaun region), Central Himalaya ($\sim$80°–89° E; Western Nepal, Central Nepal, and Eastern Nepal), and Northeast Himalaya ($\sim$89°–97° E; Sikkim, Darjeeling, Bhutan, and Arunachal Himalaya). The mega-thrusts (MCT, MBT, MFT) of the Himalayan arc pass through all of these three segments [149, 321]. Apart from this, many tear faults, splay faults, and out of sequence faults are also located in these regions.

1.4.1 Northwest Himalaya

The northwest Himalaya broadly comprises the northeastern sequence of the mountain range, longitudinal intermontane valley (e.g., Pinjore Dun and Soan Dun), the Siwalik range (e.g., Janauri anticline and Sarkaghat anticline), and the IGP in front (Fig. 1.5) [82, 164, 191, 223, 284, 290, 321]. The northeastern sequence of mountain ranges is elevated in the range of $\sim$800–2000 m and contains early to late Tertiary sedimentary rocks from Siwalik mountains that are folded and deformed by the mega thrusts [82, 196, 223]. In the Kashmir and Himachal region along the northwest Himalaya, the MBT and MCT are not well established though there are some evidences of imbricate faults (Fig. 1.5) [321]. However, along the Garhwal-Kumaun Himalaya, the region between the MBT and MCT is wider (>80 km), and both of the thrusts exhibit several surface exposure (Fig. 1.5) [321]. In the Shimla region, an exposure of the MCT, known as the Shimla Klippe, has been identified [321].

Further, the southernmost frontal thrust (MFT) makes a boundary between Quaternary fluvial deposits of the IGP and the Janauri anticline [139, 160, 191, 226]. The $\sim$170 km long Janauri anticline is bounded by the MFT in south and a south-dipping back-thrust in north [164]. In the north of the Janauri anticline, a $\sim$90 km wide convex U-shaped structure, known as the Kangra reentrant, is identified [59, 223, 269]. This region has experienced a large event in 1905 (Kangra earthquake M_w=7.8) (Fig. 1.5). Out of sequence faulting (Jawalamukhi Thrust (JMT)) along this zone has also been identified [65, 59]. Another similar reentrant, known as the Dehradun reentrant, was also found in the Dehradun region of the Garhwal Himalaya [65, 223]. It has a roughly folded zone (Santaurgarh anticline) in the north along with a broad folded southern zone (Mohand anticline) [223]. In the southeast direction of the Dehradun reentrant, the Siwalik range

narrows down and Lesser Himalaya spreads wider, and the imbricate faulting shows predominance [223].

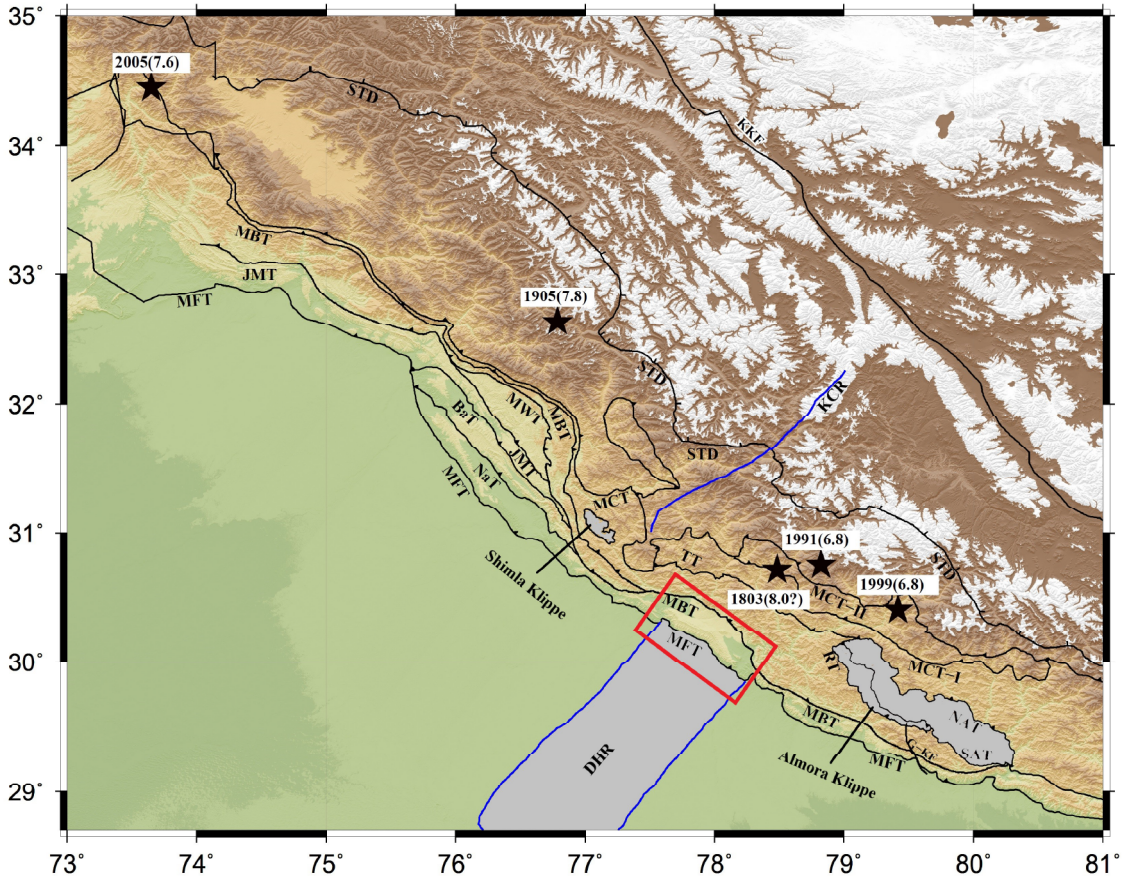

Fig. 1.5: Topographic map of the northwest Himalaya. Red rectangle represents the cusp along the MBT due to the contact of DHR. Abbreviations are as follows: BaT, Barsar Thrust; DHR, Delhi-Haridwar Ridge; G-KF, Garampani-Kathgodam Fault; JMT, Jawalamukhi Thrust; KCR, Kaurik Chango Rift; MBT, Main Boundary Thrust; MCT, Main Central Thrust; MFT, Main Frontal Thrust; MWT, Medilicott- Wadia Thrust; NaT, Nalagarh Thrust; NAT, North Almora Thrust; RT, Ramgarh Thrust; SAT, South Almora Thrust; STD, South Tibetan Detachment; TT, Tons Thrust.

These reentrants show fault-propagation folds with steep limbs in north and fault-bends along with fault propagation with gentle north dipping limbs in south [223]. In the northeast of the Dehradun reentrant, a crystalline formation of the Lesser Himalaya, known as the Almora Klippe, has been identified (Fig. 1.5). This Klippe roots into MCT in the northern side and is bounded by two imbricate faults, namely the North Almora

Thrust (NAT) in the north and the South Almora Thrust (SAT) in the south (Fig. 1.5) [290, 321].

In the north, the KCR is considered to be the most active rift among all rifts (Fig. 1.5). It controls the rupture extent of large earthquakes and influences the seismicity of the Himalayan Seismic Belt (HSB) along the northwest Himalaya [84]. The large subducting DHR may also influence seismic activity along the KCR (Fig. 1.5)[84]. The DHR represents Aravalli mountain belt's extension, and it propagates under the Himalayan arc. This propagation might associate lower magnitude seismic activity [84].

1.4.2 Central Himalaya

The central Himalaya covers the Nepal Himalaya and the southern Tibet (Fig. 1.6). The Siwalik group forms a folded Cenozoic piedmont region along the central Himalaya [290]. The megathrust system of the Himalaya has a clear demarcation in this region (Fig. 1.6) [321]. The Higher Himalaya comprises ∼10 km thick succession of crystalline rocks and fossiliferous sedimentary rocks in this region [124, 145].

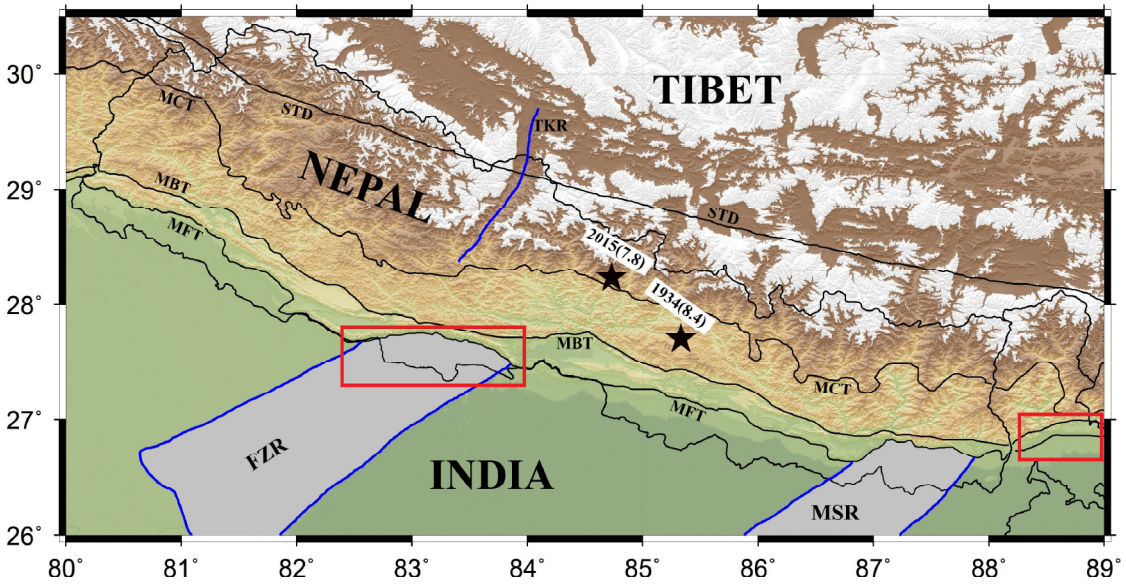

Fig. 1.6: Topographic map of the central Himalaya. Red rectangles represent the cusps on the MFT due to contact of Faizabad Ridge (FZR) and the Munger-Saharsa Ridge (MSR). Abbreviations are as follows: MBT, Main Boundary Thrust; MCT, Main Central Thrust; MFT, Main Frontal Thrust; STD, South Tibetan Detachment; TKR, Thakola Rift.

The world's highest mountain, the Mount Everest (∼8,849 m), is located in this region. The Lesser Himalaya in this part consists of the un-fossiliferous sedimentary and meta-sedimentary rocks of Precambrian to Miocene age [320]. The major formations in the central Himalaya are the Kathmandu Nappe (∼3−4 km thick Lower-Paleozoic Himalayan strata), Dadeldhura Klippe (a synformal klippe that is a continuation of the Almora Klippe in the east direction), and the Jajarkot Nappe that represents the lowest metamorphic grade exposures of the Himalayan orogeny [320, 208]. The folding of the Kathmandu Nappe suggests thrust duplexing along the ramp of the MHT in the central Himalaya [40, 154]. Due to this duplexing, the ramp of the MHT propagates southward and abandons the succession of blinds thrust in this region [40].

The central Himalaya also includes the Faizabad Ridge (FZR), a subsurface extension of the Bundelkhand massif. (Fig. 1.6) [84]. The low magnitude seismicity is evident from a densely installed seismic network along this ridge [2]. This ridge detaches Gandak depression in the east from Sarda depression in the west [84]. Like the KCR appears to align with the DHR in the northwest Himalaya, the Thakola Rift (TKR) seems to align with the FZR in the central Himalaya (Fig. 1.6) [84]. The TKR is not as active as the KCR, though it is believed that the TKR had stopped the rupture extent of the 1934 Nepal-Bihar great earthquake to further propagate in the west [84].

1.4.3 Northeast Himalaya

The northeast Himalayan range and its surrounding zones represent a complex tectonic behavior with high seismicity (Fig. 1.7). It falls in the seismic zones IV and V on the seismic zonation map of India [37]. The frontal part of the northeast Himalaya, along the Brahmaputra Basin, is jawed between the Himalayan arc and the Indo-Burmese arc (Fig. 1.7) [130]. This region has experienced two great events, namely the 1897 Shillong (M_w=8.2) earthquake and the 1950 Assam (M_w=8.6) earthquake along with several major events in the last century (Fig. 1.7). The 1897 Shillong event has occurred along the Shillong Plateau (SP) [130]. The SP is an uplifted horst block (pop-up structure), formed during the Cenozoic period and disjointed from peninsular India by Tertiary Ganges-Brahmaputra fluvial deposits [193]. The Plateau is bounded by the Dauki Fault, Dhubri fault, and the Kopili fault in the south, west, and east, respectively (Fig. 1.7) [130]. The Mikir Hills are separated from the Shillong Plateau by the Kopili fault (Fig. 1.7). The granitoid sedimentary rocks of the Mikir Hills are un-deformed and stable with no further orogenic activity [193]. The eastern boundary of the northeastern Himalaya is bounded

by the Indo-Burma Range (IBR). The IBR is a north-south trending curved thrust-fold belt and it is subdivided into Naga Hills, Manipur Hills, Chin Hills, and the Arakan-Yoma subduction belt (Fig. 1.7) [131, 193].

Further, the IBR, comprising several northeast−southwest trending strike-slip Sagaing fault, Arakan-Yoma subduction belt, Eastern Boundary Thrust, and Volcanic line, has experienced frequent normal and strike-slip events at a shallower depth and thrust events at a deeper depth (Fig. 1.7) [23]. The Indo-Burma region and the eastern Himalaya together form the Assam Syntaxis containing the Naga thrust and the Disang thrust [23, 193].

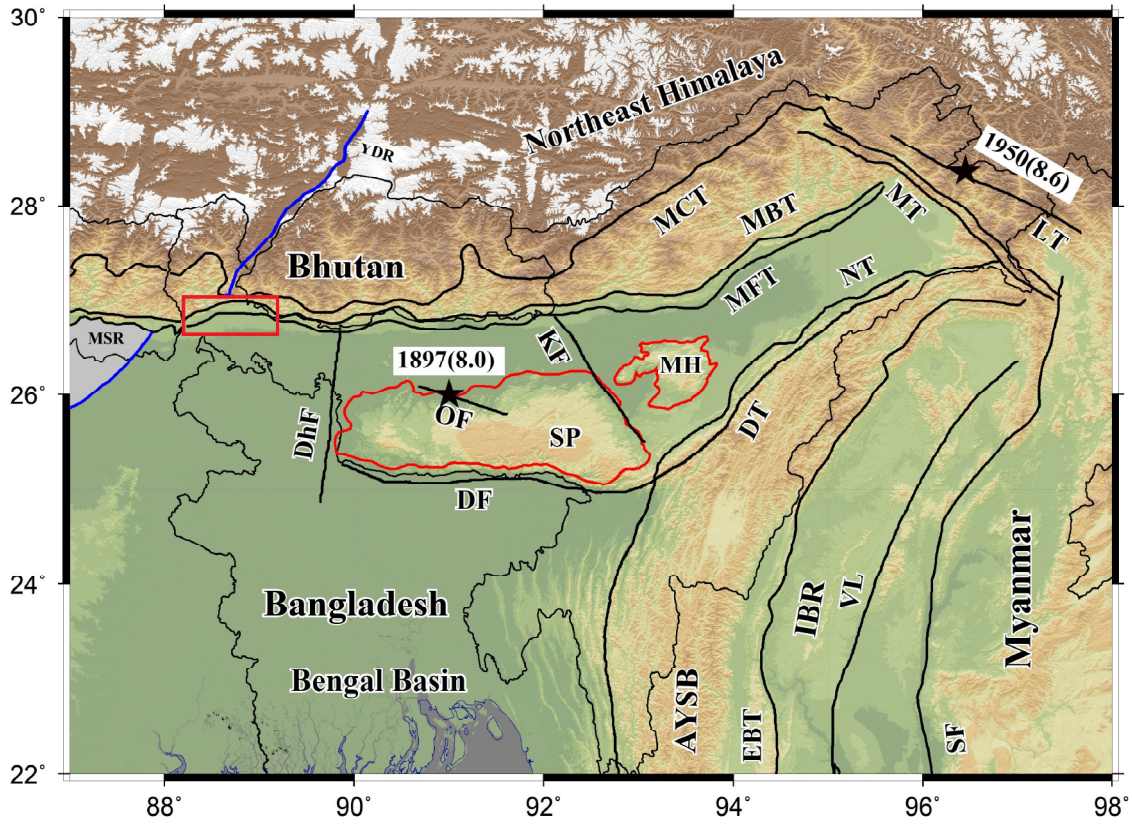

Fig. 1.7: Topographic map of the northeast Himalaya. Red rectangle represents the cusp on the MFT due to the contact of the MSR. Abbreviations are as follows: AYSB, Arakan-Yoma Subduction Belt; DF, Dauki Fault; DhF, Dhubri Fault; EBT, Eastern Boundary Thrust; IBR, Indo-Burma Range; KF, Kopili Fault; LT, Lohit Thrust; MH, Mikir Hills; MBT, Main Boundary Thrust; MCT, Main Central Thrust; MFT, Main Frontal Thrust; MSR, Munger-Saharsa Ridge; MT, Mishimi Thrust; OF, Oldham Fault; SF, Sagaing Fault; SP, Shillong Plateau; VL, Volcanic Line; YDR, Yodang Rift.

The northeast Himalaya also covers a longitudinal ridge, the MSR, which acts as the western boundary of this region. It comprises 2−3 km thick complex sedimentary

rocks from the Satpura fold belt of Chhota-Nagpur [84]. Similar to ridges and rifts in the northwest and the central Himalaya, the MSR is also aligned with a northern rift, known as the Yadong Rift (YDR) (Fig. 1.3) [84]. The YDR also controls seismicity in the Sikkim region of northeast Himalaya [84]. Like the TKR acts as a western barrier of the rupture extent of the 1934 Nepal-Bihar earthquake, the YDR acts as an eastern barrier of this event [2, 84].

A 'dent' or 'cusp' (outward concave) (red rectangles in Fig. 1.5, Fig. 1.6, and Fig. 1.7) in the arc is generally observed along the interaction between the elongated ridges and the subduction arc. Along the Himalayan orogeny, some apparent correlations between the arc and ridges have been identified, though no conclusive evidence is available yet (Fig. 1.3) [62, 84]. For example, in the northwest Himalaya, the DHR does not create any cusp right at the interaction with the MFT, though a ∼30 km long northward shift along the MBT is observed (Fig. 1.5) [62, 84]. In contrast to this, the FZR forms a cusp on the MFT along the Himalayan front in the central Himalaya (Fig. 1.6) [40, 84]. Like the DHR, the MSR also does not make any cusp on the MFT at the Himalayan front, though towards the east, a cusp formation is evident on the MFT along the Sikkim region of the northeast Himalaya (Fig. 1.7) [84]. It may be noted that the depth or the thickness of these ridges may vary along the strike, which could significantly affect the variation in geometry of these cusps along the Himalayan front [84]. The alignments of ridges and rifts, and the interactions of ridges with the Himalayan front suggest that these activities could have acted as a barrier for the rupture extent of past large earthquakes and could also possibly influence incoming seismicity in the Himalayan front [84].

1.5 Megathrust system of the Himalaya

The present tectonics of the ∼2400 km long Himalayan arc results from the north-south convergence between India and Eurasia continental plates since ∼50 Ma (Fig. 1.3) [321]. Due to this continuous collision, the Himalayan arc is considered to be one of the world's most seismically active zones. As the Indian plate moves towards the north, the sedimentary crustal layer gets complexly folded and continuously buckled and eventually breaks apart into different tectonic segments by faulting and thrusting mechanism [321]. Three major active thrust systems, namely the Main Central Thrust (MCT), the Main Boundary Thrust (MBT), and the Main Frontal Thrust (MFT), along with some imbricate branching faults and out-of-sequence faults have evolved as a result of this persistent collision (Fig.

1.4) [183, 191, 312, 321]. Further, these three megathrusts are considered to converge into a basal décollement, namely, the Main Himalayan Thrust (MHT), along which the Indian plate subducts beneath the Eurasian plate (Fig. 1.4) [290, 322].

1.5.1 Main Central Thrust

The MCT has evolved in the early Miocene period and it dips about $12^{\circ}-35^{\circ}$ in the north direction (Fig. 1.4) [283, 321]. For instance, in the Garhwal-Kumaun region, the MCT splays into the Munsiari thrust, known as the MCT-I and the Vaikrita thrust, known as the MCT-II (Fig. 1.5) [280, 321]. Two branching faults of MCT-I, namely the Ramgarh Thrust (RT) and the Almora Thrust (AT), have also been identified in the Kumaun region (Fig. 1.5) [321]. The AT which bounds the crystalline Almora Klippe in the Kumaun region is described as the South Almora Thrust (SAT) in the south and the North Almora Thrust (NAT) in the north (Fig. 1.5) [69, 221, 267]. The NAT in Garhwal Himalaya transforms into the Tons Thrust (TT), which further converges into MCT in the eastern Himachal region (Fig. 1.5) [281]. In the west, along the Himachal Himalaya, the detailed structure of the MCT is not well constrained as it is located very close to the MBT (Fig. 1.5) [321]. Yet, the presence of the MCT Klippe in Shimla, known as Shimla Klippe, has been recognized (Fig. 1.5) [147, 148, 262, 321]. The activeness of MCT is yet debated. Based on the observations of carbon dating on Quaternary deposits along the northwest Himalaya, Nakata (1989) [191] suggested that the MCT is dormant. In contrast, based on large geodetic strain rates and microseismic activity in the MCT zone along the Kumaun Himalaya, Ponraj et al. (2010) [221] suggested that the MCT is probably active. Apart from this, seismic clusters of moderate-sized earthquakes have also been identified along the MCT in the Higher Himalaya by Mukhopadhay (2011) [184].

1.5.2 Main Boundary Thrust

The MBT is a $30^{\circ}-50^{\circ}$ north dipping thrust fault, disconnecting the metasedimentary rocks of the Lesser Himalaya to unmetamorphosed classic rock deposits of the Siwalik Himalaya (Fig. 1.3). Several imbricate faults of MBT have also been traced in the west of the Himachal region, namely the Jawalamukhi Thrust (JMT), Nalagarh Thrust (NaT), and the Barsar Thrust (BaT) (Fig. 1.5) [15, 282]. Generally, the MCT is known as the ductile shear zone, whereas the MBT is characterized as a brittle fracture [290]. Along the whole central Himalaya, the MBT is so well-exposed that it can also be observed in

aerial photographs. The MBT is also penetrable on the surface of Tista River Valley in the fold-thrust belt of the Darjeeling region along the northeast Himalaya (Fig. 1.7) [186]. Though the MBT is a compressive tectonic fracture, some evidences of extension along the MBT are found [191, 192, 317]. Apart from this, in Kumaun Himalaya, the MBT has also registered rotational and strike-slip motion in Holocene time [289]. The distance between MFT and MBT varies from ∼30 km to ∼80 km in the northwest Himalaya due to the presence of large reentrants of the MBT, such as the Kangra reentrant and the Dehradun reentrant (Fig. 1.5) [321].

1.5.3 Main Frontal Thrust

In the Himalayan thrust fault system, the MFT is the most exposed and the most studied fault because of its accessibility and a warmer climate than the Higher and Lower Himalaya (Fig. 1.3) [159, 181, 321]. The MFT dips $\sim 15^{\circ}-35^{\circ}$ in the north direction and has a long-term slip rate of $\sim 8-10$ mm/yr with large uncertainties of $\sim 3-7$ mm/yr [139, 145]. It lies on the northern fringe of the IGP and marks the southern boundary of Quaternary sediments of the Siwalik Himalaya (Fig. 1.3) [182, 192, 282, 310]. Geomorphological studies along the trace of the MFT suggest that the alluvial fans and Quaternary fluvial terraces have been uplifted, indicating that MFT is highly contributing to the uplift of the Siwalik Group [191, 192, 306]. Earlier, the MFT is believed to be a zone of folds and blind thrust faults [191, 317]. However, the recent advancements of paleoseismic investigations on the MFT suggest that this fault has evidence of surface rupture and should not be treated as a dormant thrust anymore [164]. The MFT is the only thrust fault in the Himalayan megathrust system, which has provided surface manifestation of past great earthquakes along the Himalayan arc in terms of uplifted fault scarps and trenchable river terraces (Fig. 1.3) [137, 142, 162, 191, 192, 218, 305, 306, 308, 309, 317].

In the northwest Himalaya, the MFT is branched in two small subfaults, namely the HF1 and the HF2 along the northern fringe of the Janauri anticline [162, 164]. The fault scarp along HF1 is highly degraded, whereas the scarps along HF2 show younger activity with a slip rate of 7.6 ± 1.7 mm/yr [162, 164]. The Pinjore Garden Fault (PGF), a branching fault of MFT, separates the upper Siwalik Himalaya from the adjacent Pinjore dun [15]. Further, along the right side of the Gaggar riverbank, uplift scarps along the MFT have been identified and named as the Chandigarh Fault (CF) [161, 191]. At about 40 km to the southeast of the Chandigarh province, the MFT turns sharply on the right side,

near the Kala Amb province. This sharp bend is known as the Black Mango Fault (BMF), which is a tear fault of the MFT [14, 15, 161, 191]. Along the foothills of the Garhwal Himalaya, Mohand Thrust, an outlet of MFT, has deformed the Quaternary sedimentary deposits along the Dehradun region [15, 16]. In the Kumaun Himalaya, the Kaladungi Fault, a branching fault of MFT, has hosted large events between 1750 and 1932 AD [163]. Trenching excavation in the cliff of Mahara river along the Central Himalaya suggests that the MFT is splitted into two branching faults, namely Bardibas Thrust and Patu Thrust [251]. These thrusts revealed surface rupture during two events in 1255 and 1934 AD [209, 251]. Along the MFT in the northeast Himalaya, several discontinuous fault scarps have been excavated, suggesting the occurrence of paleo-earthquakes in this region [140, 172].

1.5.4 Main Himalayan Thrust

The above megathrust system in Himalaya (i.e., MCT, MBT, and MFT) is assumed to emanate from the top and merge beneath the Himalaya at $\sim$20–25 km depth into a décollement, known as the Main Himalayan Thurst (MHT) (Fig. 1.4) [194, 321, 322]. In other words, the MCT, MBT, and the MFT are considered as the splay faults of the MHT (Fig. 1.4) [94]. The MHT serves as an interface between the downgoing Indian plate and the overriding Himalayas [290, 322]. The shape of this décollement is represented as a flat-ramp-flat structure, where the mid-crustal ramp is dipping with $\sim 5^{\circ}$–15° dip angle in the north direction [2, 94, 154, 219, 277, 316]. The ramp of the MHT has hosted many large Himalayan earthquakes [2, 94, 154, 196, 219, 320]. Previous geodetic studies [e.g., 20, 88, 154, 277, 316] have suggested that the deeper part of the MHT is creeping (slow or low continuous activity occurring on a fault due to crustal deformation and because of the creeping, the fault is incapable to host large events), whereas the shallower part (i.e., MFT) is locked with a slip deficit rate of $\sim$14–18 mm/yr. This deficit rate accumulated over a century is sufficient to produce a great Himalayan earthquake in the near future [30, 154, 276].

1.5.5 Out of sequence faults

Along the collision boundary, foreland to hinterland propagation of crustal dislocations exhibits in-sequence deformation [183]. The deviation from this in-sequence deformation could appear in terms of branching, late-sequence deformation, or out-of-sequence

faulting [47, 237]. The common manifestation of out-of-sequence can be characterized by thrust faulting, strike-slip deformation, or normal folding and fracturing [183]. Out-of-sequence thrusts can be created due to the reactivation of fold-thrust wedge. Vice-versa, the fold-thrust can be reactivated through the out-of-sequence thrusts [185]. The creation of the out-of-sequence faulting on the wedge boundary may be considered to be a random process and may appear on a flat geometry of a fault system with a flat-ramp structure [230]. Below a brief discussion on the out-of-sequence faults along the Himalayan arc is provided.

In the north of the Kangra reentrant, the $\sim 30^{\circ}-50^{\circ}$ north dipping Medlicott–Wadia Thrust (MWT) is an out-of-sequence thrust that emerges into the MHT at about 10–15 km depth (Fig. 1.5) [70, 296, 297]. The MWT has several branching faults, namely the Balakot-Bagh Fault (BBF), Bilaspur thrust, Riasi thrust, and the Nahan thrust along the Siwalik Himalaya. These faults have evolved during the late to early Quaternary–Holocene period [282, 296]. The BBF hosted the 2005 Kashmir earthquake in the northwest Himalaya [106]. In the northwest Himalaya, the BBF with a slip rate of 1.4–4.1 mm/yr is observed to cut MCT and MBT, though it does not converge up to the MFT [128]. The BBF is reported to be the continuation of the Kashmir Basin Fault (KBF), which further transforms into a right-lateral strike-slip fault, the Central Kashmir Fault (CKF) [4, 128, 260]. Adjacent to the CKF, the Riasi thrust is a $\sim$70 km long and $\sim 50^{\circ}$ northeast dipping fault which consumes $\sim$50% of crustal shortening along the Kashmir Himalaya with a total slip rate of 6.4 ± 2.9 mm/yr [89]. The 14 ± 1 mm/yr of slip deficit rate on the Bilaspur thrust suggests the possibility of a great earthquake in the near future [122]. The Nahan thrust along the Siwalik Himalaya shows $\sim$10 mm/yr of slip rate [270]. In the upper Lesser Himalaya, the dextral strike-slip fault, the Kangra Valley Fault (KVF), is suggested to be the epicentral source of the 1905 Kangra earthquake [163]. In addition, the MFT and the MBT in the Nainital region are right laterally offset by a strike-slip fault, the Garampani-Kathgodam Fault (G-KF), which is observed to extend from Rampur thrust in the north to the IGP in the south (Fig. 1.5) [318]. Along the Siwalik groups of the central Himalaya, a series of $40^{\circ}-50^{\circ}$ dipping Main Dun Thrusts (MDT) is identified between the MBT and the MFT [107, 178, 182]. In the northeast Himalaya, the Kopili Fault (KF) is a northwest–southeast trending strike-slip fault (Fig. 1.7) [263]. Intense seismic clusters have been observed at a seismogenic depth of $\sim$50 km of the KF and this seismicity continues to further north up to the MCT [263]. In the west of the KF, the 1897 Shillong earthquake was hosted by a south-dipping reverse fault, the Oldham Fault (OF), located

in the north of the Shillong Plateau (Fig. 1.7) [75]. The northeastern Himalayan zone also includes some out-of-sequence faulting, such as the northwest–southeast trending Mishmi Thrust (MT) and Lohit Thrust (LT) (Fig. 1.7) [23, 193]. Nonetheless, the out-of-sequence faulting has existed throughout the entire length of the Himalayan arc and has hosted previous large earthquakes. Therefore, the possibility to host upcoming large events on these out-of-sequence thrusts is also undeniable [17, 183].

1.6 Seismicity along the Himalaya

The continuous convergence of Indian and Eurasian plates causes enormous stress accumulation along the Himalayan arc, which has in turn produced several moderate to great earthquakes in the past (Fig. 1.8) [2, 30, 34, 154, 277, 290]. The below sections provide some discussions on the important paleo and medieval age, pre-instrumental, and instrumental seismicity, with an emphasis to the great Himalayan earthquakes.

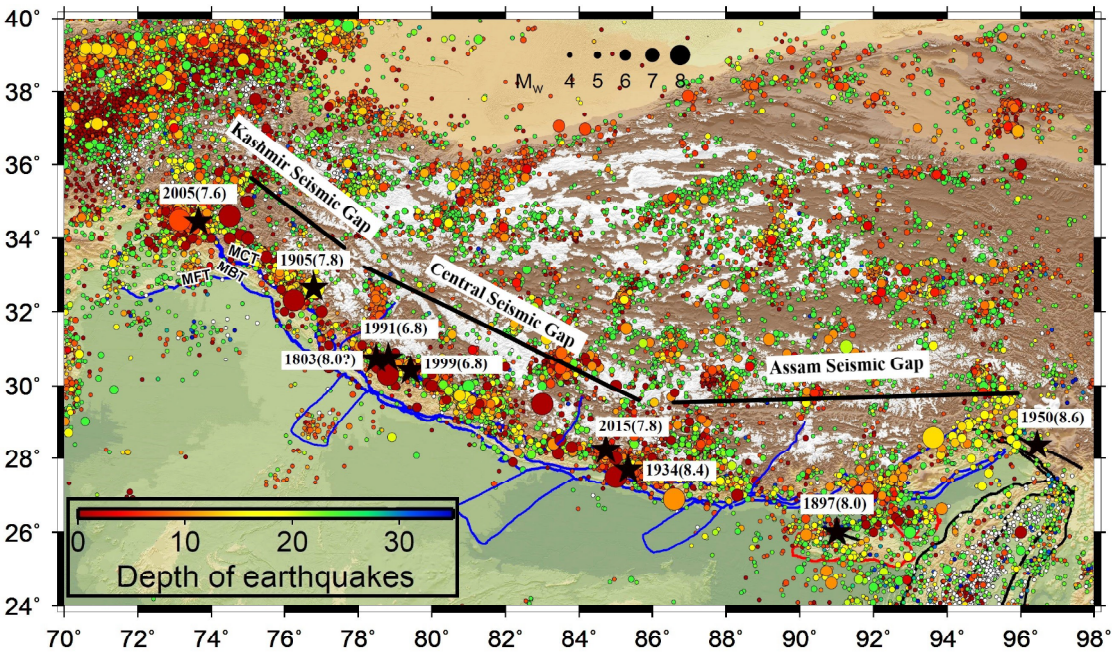

Fig. 1.8: Seismicity of the Himalaya. Abbreviations are as follows: DHR, Delhi-Haridwar Ridge; FZR, Faizabad Ridge; MBT, Main Boundary Thrust; MCT, Main Central Thrust; MFT, Main Frontal Thrust; MSR, Munger-Saharsa Ridge.

1.6.1 Paleo and medieval earthquakes

It has been observed that more studies on paleo and medieval earthquakes have been conducted along the central Himalaya in comparison to the northwest and northeast Himalaya [30, 129]. The earliest giant earthquake of magnitude 8.5$\leq M_w \leq$9.0 [30] occurred in 1100 AD along the central Himalaya with the lateral extent and surface deformation of $\sim$240 km and $\sim$17$\pm$4 m, respectively [146, 305]. The second studied mega-event of 7.5$\leq M_w \leq$8.5 [30] occurred in 1225 AD along the Kathmandu region of the central Himalaya. It is also reported that this event killed one-third population of the Kathmandu region [30, 209, 251]. In 1344 AD, one more mega-earthquake struck along the central Himalaya with size, rupture length, and an average slip of $M_w \geq$8.5, $\sim$600 km, and $\sim$15 m, respectively [229]. In 1505 AD, another intense event occurred along the central Himalaya (around the central to western Nepal region and Kumaun Himalaya region) with a maximum slip of 10$-$15 m and magnitude of 8.7$\leq M_w \leq$8.9 [7, 30, 40, 163, 305, 306]. This earthquake produced surface rupture of $\sim$100 km in width and 450$-$500 km in length along the central Himalaya. Evidence of surface ruptures was found in the IGP across the MFT [7, 30, 40, 305, 306]. The 1555 AD (7.6$\leq M_w \leq$8.0) event with a rupture length of $\sim$170 km and slip of 2$-$5 m killed thousands of people in the Kashmir region of the northwest Himalaya [7, 30].

1.6.2 Pre-instrumental earthquakes

A great earthquake of 8.0$\leq M_w \leq$8.2 [30] ruptured in 1741 AD along the Bhutan Himalaya with a slip of 4.5$-$5.0 m. The first nineteenth-century great earthquake (1803 Garhwal earthquake) was observed in the western rupture end of the 1505 AD earthquake (Fig. 1.8). This event had a rupture length of $\sim$200 km on the MFT with an average slip of 4.5$-$5.0 m. Severe damage was observed in the Garhwal region, killing hundreds of people and destroying thousands of houses [30]. Before 1897, all of the great earthquakes are known from their felt effects and damages, in which the exact magnitudes are mostly unavailable [30]. However, the spatial distribution of the intensities for these earthquakes is available, from which the possible magnitude ranges can be estimated [30, 129]. The great 1897 Shillong Plateau earthquake of $M_w \geq$8.2 is the first event that was extensively studied by geologists and geophysicists, and was recorded by several seismometers in Europe (Fig. 1.8) [30, 201]. This event produced a 500 km long and 300 km wide rupture zone and nucleated in the south of the Himalayan front [30, 259]. There were 1,542

human deaths and many masonry buildings were destroyed over a region of 400,000 km^2 [30, 259].

The April 04, 1905 Kangra earthquake was the first twentieth-century disastrous earthquake that occurred in the Himalayan orogeny (Fig. 1.8) [30, 301]. This damaging seismic activity caused more than 20,000 casualties and vanished 100,000 houses around the Kangra valley [30, 301]. The recent assessments on the 1905 Kangra earthquake suggest that the size, maximum slip, and rupture length of this event were M_w=7.8, 7 m, and ∼150 km, respectively [301]. The January 15, 1934 Nepal-Bihar earthquake caused extensive damages in northern Bihar and Nepal, resulting in 10,600 deaths and collapsing a large number of dwellings (Fig. 1.8) [207]. Strong shaking and damages were reported far from Tibet, Mumbai, Assam, Punjab, and the West Bengal [193]. The rupture length and the maximum slip of this great earthquake (M_w=8.4) were ∼200−300 km and 6 m, respectively [94, 207].

1.6.3 Instrumental earthquakes

The August 15, 1950 Assam earthquake of magnitude M_w=8.6 struck in the easternmost boundary of the Himalayan arc (Fig. 1.8) [193]. This earthquake produced 250 km of surface rupture and a slip of 5.5±0.7 m, killing ∼4,800 people in this region [224]. Apart from this, two strong events, namely the 1991 M_w=6.8 Uttarkashi earthquake and the 1999 M_w=6.8 Chamoli earthquake have also occurred along the Garhwal-Kumaun region of northwest Himalaya in the late 20^{th} century (Fig. 1.8) [129]. These earthquakes were also located around the construction site of the Tehri-dam in the northwest Himalaya [30, 129].

The October 08, 2005 Kashmir earthquake of magnitude M_w=7.6 ruptured ∼75 km long stretch with an average slip of ∼4.2 m in the Muzaffarabad region of northwest Himalaya, damaging many areas of Pakistan and Jammu-Kashmir of India (Fig. 1.8) [128, 231]. It occurred at 8.40 am (regional time), when various poorly constructed schools and other government to private institutions were occupied. The earthquake killed more than 80,000 people and razed millions of constructions [128, 231]. The most recent earthquake, the April 25, 2015 Gorkha earthquake (M_w=7.8) has ruptured at about 60 km far from the Kathmandu valley of the central Himalayan range (Fig. 1.8). This event has a rupture length of ∼150 km and a maximum slip of ∼6 m. The epicenter of this event was near the northwestern boundary of the rupture zone of the 1934 Nepal-Bihar earthquake

(Fig. 1.8) [30, 72, 316]. About 8,964 people have lost their lives, ∼21,952 were seriously injured, and about 3.5 million houses were destroyed during this event [30].

1.7 Seismic gaps along the Himalayan arc

The seismic gap hypothesis stems from the concept of the "elastic rebound theory"[234]. This theory states that continuous stress by the plate motion along a fault or a plate boundary results into the accumulation of strain energy until the strength of internal rocks exceeds [234]. The strain energy accumulated over the years releases through earthquakes, and the rocks come back to their normal shape [234]. As a consequence, the section of a plate boundary which has not released any seismic rupture or strain energy for a long time, though it is capable of, is marked as "seismic gap" [125, 126, 238, 255]. On the basis of the spatial distribution of great Himalayan earthquakes and their long quiescence in highly hazardous segments, three broader seismic gaps have been identified, namely the Kashmir seismic gap, central seismic gap, and the Assam seismic gap (Fig. 1.8) [93, 132, 133, 273].

In the west, the Kashmir seismic gap lies in the western end of the rupture zone of the 1905 Kangra earthquake (Fig. 1.8) [273]. The 2005 Kashmir earthquake occurred at the western boundary of the Kashmir seismic gap [273]. In the center lies the largest seismic gap (∼600 km), known as the central seismic gap (Fig. 1.8). It is located between the rupture zones of the 1905 Kangra earthquake and the 1934 Bihar-Nepal earthquake (Fig. 1.8) [132, 133]. The region is considered to be the most likely segment waiting for a great earthquake ($M_w \geq 8.0$) [93, 132, 133, 273]. However, this postulated seismic gap concept is highly debated [7, 227], as two significant historical earthquakes are found to occur in this region, in AD 1505 and 1803 (Fig. 1.8). Thus, occurrences of these events raised the question about the validity of the central Himalaya being a seismic gap [7, 227]. In the east of the central seismic gap lies the Assam seismic gap between the rupture zones of the 1934 Nepal-Bihar earthquake and the 1950 Assam earthquake (Fig. 1.8) [93, 273]. The possible recurrence of large earthquakes along the locked portion of MHT is often discussed in light of these seismic gaps along the entire Himalayan belt [7, 93, 125, 126, 273].

Till now, a thorough discussion on the evolution of the Himalaya, Himalayan tectonics, longitudinal and latitudinal segmentation of the Himalayan arc, Himalayan megathrust system, and observed seismicity along with the existing seismic gaps is provided.

The below section highlights the research objectives and scope of the present thesis.

1.8 Thesis objective

The main objective of the thesis work is to characterize interseismic crustal deformation and consequently to re-evaluate contemporary earthquake potential along the Himalayan arc. To achieve this main objective, three sub-objectives are framed below.

1. To derive the updated crustal deformation field (i.e., surface velocity and strain rate distribution) along the Himalayan arc utilizing the new and published GPS data
2. To model the updated fault kinematics (i.e., slip rate distribution and fault geometry) of the Himalayan megathrust system
3. To estimate the spatial distribution of contemporary earthquake potential along the Himalayan arc

1.9 Scope of the thesis

This section explains various scopes and key work elements to accomplish the above mentioned research goal.

1. Permanent/campaign GPS data collection at each site of the regional network comprising three arc-normal transects and one arc-parallel transect.
2. GPS data processing using GAMIT-GLOBK suite of post processing software.
3. Plotting the position time-series and velocity vectors.
4. Combining the regional velocity vectors (40 GPS velocity data) with published velocity vectors (446 GPS velocity data) in a common reference frame using a seven parameter Helmert transformation.
5. Computing the strain rate distribution (dilatation, maximum shear, and rotation strain rates) using the updated surface velocity field.
6. Calculating the slip rate and fault geometry of the Himalayan megathrust system by inverting horizontal velocities using a two-dimensional Bayesian splay-fault inversion model.

7. Evaluating geodetic moment rates from strain rates and seismic moment rates using historical seismicity data.

8. Estimating spatial distribution of earthquake potential along the Himalayan arc by comparing geodetic and seismic moment rates.

9. Computing natural time statistics of populous cities along the Himalayan subcontinents and further estimating earthquake potential scores for these cities using a number of probability models.

10. Identifying the regions of high seismic hazard along the Himalayan arc from a combination of geodetic and statistical approaches.

1.10 Structure of the thesis

The present thesis focuses on the characterization of the ongoing crustal deformation and consequent earthquake potential along the Himalayan orogeny. The thesis is organized into seven chapters.

Chapter 1 provides a theoretical overview of the Himalayan arc in terms of evolution, tectonics, subdivisions, seismicity, and existing seismic gaps. In addition, this chapter includes thesis objectives and a brief summarization of the thesis road map.

Chapter 2 covers an explicit literature review on seismic hazard studies along the Himalayan arc. The literature survey of geological and geodetic studies is carried out for northwest, central, and northeast Himalaya. The chapter concludes with a comparison of geological findings and geodetic results along the Himalayan arc.

Chapter 3 presents a brief overview of the GPS basics, GPS data collection and its processing with GAMIT-GLOBK software, coordinate time series, and the crustal deformation field in terms of surface velocity and strain rate distribution.

Chapter 4 determines the spatial distribution of slip rate and fault geometry of the Himalayan megathrust system using splay-fault Bayesian inversion model. The chapter concludes by computing the earthquake potential from the derived slip deficit rates.

Chapter 5 focuses on the computation of the spatial distribution of earthquake potential by comparing the accumulated geodetic moment rates (calculated from strain rates) with the associated released seismic moment rates (calculated from $\sim$900 years of seismicity data) along different segments of the Himalayan arc.

Chapter 6 presents an empirical data-driven technique, known as earthquake nowcasting, to statistically address the current state of regional earthquake hazard at a dozen populous cities along the Himalayan subcontinent.

Finally, **Chapter 7** summarizes the thesis work with an emphasis to the major contributions and future recommendations.